

## Marginal Instability?

S. A. THORPE

*School of Ocean Sciences, Bangor University, Menai Bridge, Anglesey, United Kingdom*

ZHIYU LIU

*School of Ocean Sciences, Bangor University, Menai Bridge, Anglesey, United Kingdom, and Physical Oceanography Laboratory, Ocean University of China, Qingdao, China*

(Manuscript received 25 September 2008, in final form 11 February 2009)

### ABSTRACT

Some naturally occurring, continually forced, turbulent, stably stratified, mean shear flows are in a state close to that in which their stability changes, usually from being dynamically unstable to being stable: the time-averaged flows that are observed are in a state of marginal instability. By “marginal instability” the authors mean that a small fractional increase in the gradient Richardson number  $Ri$  of the mean flow produced by reducing the velocity and, hence, shear is sufficient to stabilize the flow: the increase makes  $Ri_{\min}$ , the minimum  $Ri$  in the flow, equal to  $Ri_c$ , the critical value of this minimum Richardson number. The value of  $Ri_c$  is determined by solving the Taylor–Goldstein equation using the observed buoyancy frequency and the modified velocity. Stability is quantified in terms of a factor,  $\Phi$ , such that multiplying the flow speed by  $(1 + \Phi)$  is just sufficient to stabilize it, or that  $Ri_c = Ri_{\min}/(1 + \Phi)^2$ .

The hypothesis that stably stratified boundary layer flows are in a marginal state with  $\Phi < 0$  and with  $|\Phi|$  small compared to unity is examined. Some dense water cascades are marginally unstable with small and negative  $\Phi$  and with  $Ri_c$  substantially less than  $1/4$ . The mean flow in a mixed layer driven by wind stress on the water surface is, however, found to be relatively *unstable*, providing a counterexample that refutes the hypothesis. In several naturally occurring flows, the time for exponential growth of disturbances (the inverse of the maximum growth rate) is approximately equal to the average buoyancy period observed in the turbulent region.

## 1. Introduction

### a. Marginal instability

This is an examination of the hypothesis that the mean state of continually forced, naturally occurring, stably stratified turbulent flows is generally one that is marginally unstable.

The concept of control in a marginal state is introduced by Turner (1973), who refers to Mittendorf’s (1961) laboratory observations:

After the Kelvin–Helmholtz mechanism had led to the breakdown of an interface between two accelerating layers [of different densities] in an inclined tube, the turbulence in the mixing region was suppressed before

the transition layer had spread out very far. In one experiment he observed three successive breakdowns of the interfacial region, separated by quiescent periods. While turbulence is present the drag on the layers increases and the velocity falls, but when it is suppressed the flow is accelerated again by gravity. This behaviour can now be interpreted in terms of an increase of an appropriate gradient Richardson number to a stable value, because of the decrease of the velocity gradient due to mixing.

Turner goes on to discuss the Ellison and Turner (1959) experiments on the flow of relatively dense fluid cascading down a slope beneath a deep layer.

At moderately steep slopes the stress depends mostly on the entrainment at the outer edge of the layer and little on bottom friction. The turbulence effecting the entrainment is therefore produced in the same region as it is used to do work against buoyancy forces. . . . Because of the component of gravity which tends to accelerate the flow if the stress becomes too small, one might expect in addition that

---

*Corresponding author address:* S. A. Thorpe, ‘Bodfryn,’ Glanrafon, Llangoed, Anglesey LL58 8PH, United Kingdom.  
E-mail: oss413@sos.bangor.ac.uk

this outer edge could be maintained in a marginally stable state. . . The experiments support the existence of a critical gradient Richardson number, less than 0.1, at which turbulence is strongly damped.

In other words, a decrease in turbulence will lead to a reduction in the Reynolds stress in the upper region of the downslope density flow, but the downslope component of gravity will then lead to acceleration of the current, the growth of billows, an increase in turbulence, and enhanced Reynolds stress, maintaining the flow in a marginal state characterized by the gradient Richardson number.<sup>1</sup>

*b. The Taylor–Goldstein equation and the Miles–Howard theorem*

The Taylor–Goldstein (T–G) equation,

$$d^2\phi/dz^2 + \{N^2/(U - c)^2 - k^2 - d^2U/dz^2/(U - c)\}\phi = 0, \quad (1)$$

with appropriate boundary conditions, determines the stability of small disturbances in a steady, stably stratified, shear flow. In (1) the streamfunction is  $\psi(x, z, t) = \phi(z) \exp[ik(x - ct)]$ , and  $k$  is the (real) wavenumber of a two-dimensional disturbance in the horizontal  $x$  direction in which the flow has a component,  $U(z)$ . The buoyancy frequency is  $N(z)$ . The term  $c = c_r + ic_i$  is the complex wave phase speed, so that  $c_r$  is the phase speed of disturbances and  $kc_i$  is their growth rate. Effects of viscosity and diffusion are neglected. In real flows, at least those close to marginal conditions, turbulent fluxes are likely to be moderate, possibly justifying the neglect of terms representing the vertical turbulent transport of momentum and the vertical flux of buoyancy. It is important, however, to stress that we shall here examine the stability of an observed mean flow found by averaging in time over the turbulent motions and density fluctuations associated with turbulence and internal waves, and using the T–G equation neglecting terms representing turbulent fluxes. Our definition of “marginal” is therefore restricted by these constraints. It appears, however, to be the simplest and most pragmatic way to conduct an investigation of the state of an observed flow,

<sup>1</sup> It should be noted that the velocity is the main flow quantity being modulated, and that this discussion is strictly two dimensional, describing the effects of turbulence acting normal to the slope ( $z$ ) on the downslope ( $x$ ) flow, without regard to the effect of local patches of turbulence in producing different downslope speeds at different positions ( $y$ ) parallel to isobaths. How enhanced turbulence in some local region will affect the downslope flow requires consideration of the effects of variations in three dimensions.

or one that may be generated by a numerical model of a real flow.

The neglect of the turbulent fluxes implicitly constrains marginal to refer to the stability of the mean flow found by averaging over its fluctuations but assuming it is inviscid and nondiffusive. With  $U$  and  $N$  specified, the T–G equation can be solved by the shooting method (e.g., see Hazel 1972; Davis and Peltier 1976; Merrill 1977; Sun et al. 1998) or by the matrix method (Monserrat and Thorpe 1996; Moum et al. 2003) to obtain values of  $c$  for a given  $k$ , and the maximum growth rate of unstable modes can be determined. [In the appendix we derive an integral formula for  $c$ , similar to that given by Moum et al. (2003), that is useful as a check of the matrix method of solving the T–G equation.]

The Miles–Howard theorem, derived by Miles (1961) and Howard (1961) from the T–G equation, provides a sufficient condition for stability: under certain restrictive conditions, a stratified shear flow is stable if

$$\text{Ri} = \frac{N^2}{\left(\frac{dU}{dz}\right)^2} \quad (2)$$

is greater than  $1/4$  for all values of  $z$  (i.e., the minimum Richardson number,  $\text{Ri}_{\min} > 1/4$ ).

For many flows, the critical Richardson number  $\text{Ri}_c$ , the value of  $\text{Ri}_{\min}$  below which small disturbances grow, is equal to  $1/4$ ; flows in which  $\text{Ri}_{\min}$  is less than  $1/4$  will then be unstable with exponentially growing disturbances. Eriksen (1978) and Davis et al. (1981) show scatterplots of values of  $N$  versus those of  $dU/dz$  at fixed depth in the thermocline. Values are calculated from differences of densities and velocities from pairs of instruments separated by 3–7 m in the vertical. The plots have an apparent cutoff at a ratio,  $N/(dU/dz)$ , of about  $1/2$  (i.e., when  $\text{Ri} \approx 1/4$ ), there being relatively few measurements with smaller values of the ratio.<sup>2</sup> This is interpreted to imply that Kelvin–Helmholtz instability (KHI) is relatively rare. It appears that a value,  $\text{Ri} \approx 1/4$ , is a “critical” value in the sense that fluctuations that increase the shear,  $dU/dz$ , and reduce the vertical density gradient and therefore  $N$ , promoting local regions where  $\text{Ri} < 1/4$ , cause instability and a vertical transfer of momentum that increases  $\text{Ri}$ , bringing the flow to a stable value  $> 1/4$ . Being

<sup>2</sup> The measurements at vertically separated instruments do not resolve the micro- or fine structure of velocity and density variations, and provide only upper bounds of the minimum  $\text{Ri}$  in the water column between the pairs of instruments. The cutoff observed by Davis et al. (1981) appears closer to  $\text{Ri} = 1/8$  than the  $1/4$  value of Eriksen’s (1978) data.

mainly associated with internal waves, such regions may be identified as those of wave breaking.<sup>3</sup> The cutoff may also be interpreted to imply that, in the thermocline, the mean flow and internal wave field are in a controlled state near marginal conditions, or that the internal wave field is “saturated,” any further increase of internal wave energy resulting in wave breaking and dissipation that return the flow field toward a state with  $Ri_{\min} > 1/4$ . Except where the flow is continuously forced, for example by inertial waves (Alford and Gregg 2001) or by major currents [e.g., the equatorial undercurrent (Gregg 1976)], instability in the main thermocline is caused intermittently by the occasional arrival of groups of internal waves or the superposition of two or more internal waves, and the time-averaged flow is generally statically and dynamically stable, with a value of  $Ri_{\min}$  determined from the mean velocity and density, greater than  $1/4$ .

There are, however, flows with  $Ri_{\min} < 1/4$  that are stable (i.e., in which the critical Richardson number  $Ri_c$  is less than  $1/4$ ), and an example is described in the next section. The Miles–Howard theorem therefore provides a condition that is sufficient to ensure stability of a flow with  $Ri > 1/4$  everywhere, but does not provide what is often needed—the condition that an observed flow is definitely unstable through KHI. Nor, by itself, does the theorem provide information about the nature of unstable disturbances; this is revealed by the solutions of the T–G equation.

### c. Dense water cascading down a slope

Thorpe and Ozen (2007) solve the T–G equation by the shooting method, taking for  $U(z)$  and  $N(z)$ , data obtained during periods of cold winter weather leading to the gravity-driven cascading of cold, and therefore relatively dense, water as a density current down the 4.6° sloping bottom of Lake Geneva.<sup>4</sup> The average mean

density is statically stable (i.e., with density increasing downward) but the mean downslope flow is unstable to KHI. The most unstable disturbance is of mode 1, growing exponentially with a growth rate,  $kc_i$ , of  $1.36 \times 10^{-4} \text{ s}^{-1}$  and with a maximum amplitude at a level where  $Ri_{\min}$  is about 0.1.<sup>5</sup> The most unstable disturbance grows exponentially in a time,  $\tau = (kc_i)^{-1}$ , of 2.04 h with its maximum amplitude at a level where the buoyancy period,  $T_b = 2\pi N^{-1}$ , is about 1.4 h, giving  $\tau/T_b \approx 1.5$ .

A reduction of the observed mean flow speed at all levels, and therefore the shear, by about 20% is just sufficient to reduce the growth rate found in the T–G equation to zero (i.e., to stabilize the flow). The flow speed and shear were adjusted in accordance with the notion that, in the cases to be examined, instability is driven and controlled by flow acceleration and deceleration in the cascading flow discussed by Turner or by mechanical forcing (e.g., in section 2, by wind stress), rather than by density or buoyancy changes. We define a factor,  $\Phi$ , such that multiplying the flow speed by a factor  $(1 + \Phi)$  is just sufficient to stabilize disturbances; all solutions to the T–G equation have  $kc_i \leq 0$ : for the cascading flow  $\Phi = -0.2$ . The parameter  $\Phi$  provides a measure of the marginal condition of the flow and of the critical  $Ri$ ,

$$Ri_c = \frac{Ri_{\min}}{(1 + \Phi)^2}, \quad (3)$$

for flows with the same  $N$  and having velocity profiles with the same shape. Here  $Ri_c$  is about 0.14 (substantially less than  $1/4$ ) and in the sense that  $|\Phi|$  is small compared to unity and the growth time of disturbances is large, the flow is marginal as conjectured by Turner.

To provide a comparison for this, and later, results, we note that for unstable periodic disturbances to a shear flow at a density interface within a vertically unbounded fluid, with profiles of velocity and density being hyperbolic tangents (i.e.,  $U$  and  $\rho$  both  $\propto \tanh az$ , where  $a$  is constant), the ratio  $\tau/T_b$  is equal to 1 when  $Ri_{\min} \approx 0.18$  (Hazel 1972). The critical Richardson number  $Ri_c$  is equal to  $1/4$ , so that the value of  $\Phi$  corresponding to  $Ri_{\min}$  is  $-0.15$ . (A summary of this and other values is given in Table 1.) The buoyancy frequency represents the greatest frequency of small, localized internal waves, and so  $T_b$  represents the smallest period of these internal waves. When  $\tau/T_b \leq 1$ , exponential growth of small disturbances may occur in a time less than the period of internal waves.

<sup>3</sup> Examples of the breaking of an internal soliton wave, of the problems of adequately resolving  $Ri$  from measured data, and of the use of the Taylor–Goldstein equation to examine the stability of the wave are given by Moum et al. (2003). Laboratory experiments by Troy and Koseff (2005) and numerical calculations by Fringer and Street (2003) suggest that although unstable disturbances will begin to grow if  $Ri_{\min} < 1/4$  in internal waves traveling on a relatively thin interface, Kelvin–Helmholtz billows will not have time to form unless the wave period is sufficiently great in comparison with their  $e$ -folding time, and that a value of  $Ri_c$  near 0.1 may be a more appropriate limiting value to determine the onset of mixing caused by the overturning billows.

<sup>4</sup> Thorpe and Ozen (2007) give other examples of flows with  $Ri_c < 1/4$ . Mr. Jan Zika made a further study of a cascading flow at the Woods Hole Oceanographic Institution Geophysical Fluid Dynamics (GFD) Summer School in 2007, reaching similar conclusions to Thorpe and Ozen about its marginal stability (see Zika 2008).

<sup>5</sup> Even smaller values of  $Ri$  are found very close to the sloping boundary and below the level of the maximum downslope velocity, where  $Ri$  tends to infinity.

TABLE 1. Summary table showing the critical value of  $Ri$  ( $Ri_c$ ), the minimum observed  $Ri$  ( $Ri_{\min}$ ), the ratio of the  $e$ -folding times of the most unstable disturbances to the buoyancy period ( $\tau/T_b$ ), and the value of  $\Phi$  for flows of different sources discussed in text. The data for the atmospheric boundary layer are from Merrill (1977), those for the Equatorial Undercurrent are from Sun et al. (1998), and those for the Clyde Sea are from Liu (2009).

Source	$Ri_c$	$Ri_{\min}$	$\tau/T_b$	$\Phi$
tanh profiles (section 1c)	0.25	0.20	1.51	-0.016
	—	0.18	1.05	-0.152
	—	0.15	0.69	-0.225
	—	0.10	0.40	-0.368
Cascade (section 1c)	0.16	0.1	1.5	-0.2
Atmospheric BL (section 1d)	$\leq 0.25$	0.15	1.5	-0.23 to 0
Loch Ness surface BL (section 2)	$0.25 \pm 0.11$	0.012	0.65	$-0.78 \pm 0.05$
Equatorial Undercurrent (section 3)	$\leq 0.25$	0.13	1.1	-0.28 to 0
Clyde Sea (hour 15; section 3)	$0.21 \pm 0.04$	0.02	0.17	$-0.69 \pm 0.03$

#### d. The atmospheric boundary layer

Merrill (1977) examines the stability of the mean wind and temperature profiles averaged over a period of 10 min in a 200-m-deep, stably stratified, nocturnal atmospheric boundary layer. The minimum  $Ri$  is 0.15 at a height of about 110 m where the shear is approximately uniform in height with  $dU/dz \approx 0.071 \text{ s}^{-1}$ , implying (since  $Ri_{\min} \leq Ri_c \leq 0.25$ ) that  $0.6 \leq Ri_c/Ri_{\min} \leq 1$  and  $-0.225 \leq \Phi \leq 0$ , close to marginal conditions. Merrill solves the T–G equation (incorporating the mean profiles) by the shooting method. Unstable disturbances are found with an exponential growth period  $\tau$  of 286 s, giving  $\tau/T_b \approx 1.5$ , where  $T_b$  is the buoyancy period at 110 m. They have phase speeds of 6–6.5  $\text{m s}^{-1}$  and wavelengths of 370–1250 m, with maximum growth rate for a wavelength of 640 m. These calculated values compare with microbarograph and acoustic sounder records of tilted braidlike disturbances (microfronts or temperature ramps) attributed to KHI with a mean phase speed of 7–9  $\text{m s}^{-1}$  and wavelength (inferred from phase speed and period) of 340–450 m. Linear stability theory—the use of the T–G equation with its implicit neglect of viscosity and diffusion—accounts moderately well for the generation of the observed oscillations.

We now test (and refute) the hypothesis that boundary layer flows are always marginal by examining a further, but different, example of a stratified boundary layer flow. It is one driven by the wind on the water surface.

## 2. The near-surface boundary layer

Thorpe and Hall (1977) solve the T–G equation by the shooting method to examine the stability of the average of two vertical profiles of horizontal velocity and density made in the freshwater lake, Loch Ness, in Scotland in July 1976. The parameter  $\Phi$  is not determined, but the flow is unstable with the fastest growing disturbances in the limited range examined (40–140 m) having a wavelength of

about 60–125 m, a range covering the distance between temperature ramps determined from their repetition period in the known mean flow. The  $e$ -folding time scale of the fastest growing disturbances exceeds 1 h ( $\tau/T_b > 7.5$ , where  $T_b$  is the mean buoyancy period in the mixed layer). An increase in mean flow (or of the shear) of 5% (a value  $\Phi = 0.05$ ) is sufficient to result in the growth of periodic disturbances with a length of 63 m (roughly that of the ramps) in an  $e$ -folding time of 22.4 min ( $\tau/T_b \approx 2.9$ ). The uncertainty of estimates of growth rates in a mean flow that is determined from only two profiles is, however, considerable and the analysis is therefore unsatisfactory and inconclusive.

We have therefore conducted a more thorough investigation of the stability of wind-driven flow near the water surface by examining the flow shown in Fig. 1, the mean of 25 profiles of velocity and density in Loch Ness measured over a different daytime period of about 7 h in September 1973. [The series of profiles are shown in Fig. 18 of Thorpe (1977), where details of the measurement technique are given.] The speed of the wind along the loch axis decreased gradually from about 8.5 to 6.5  $\text{m s}^{-1}$  during the period. Whitecapping was frequent, with wave heights of about 0.6 m and periods of 3 s. The sky was overcast with air temperature about 1.5°C greater than the surface water temperature; the air–water heat flux was not measured but was probably small and positive. Except for a slow rise in isopycnals at a rate of about 0.2  $\text{m h}^{-1}$ , the measured flow conditions in the loch remained fairly steady.

The two components of the averaged flow shown in Fig. 1a are  $U(z)$ , in the wind direction parallel to the axis of the loch, and  $V(z)$ , across the loch to the right of the wind. The strength and direction of the mean current varied in depth, being 0.201  $\text{m s}^{-1}$  in a direction 20° to the right of the wind direction near the surface, and in the wind direction from about 12 to 18 m, where  $V$  was very small. The mean density  $\sigma_T(z)$ , derived from temperature

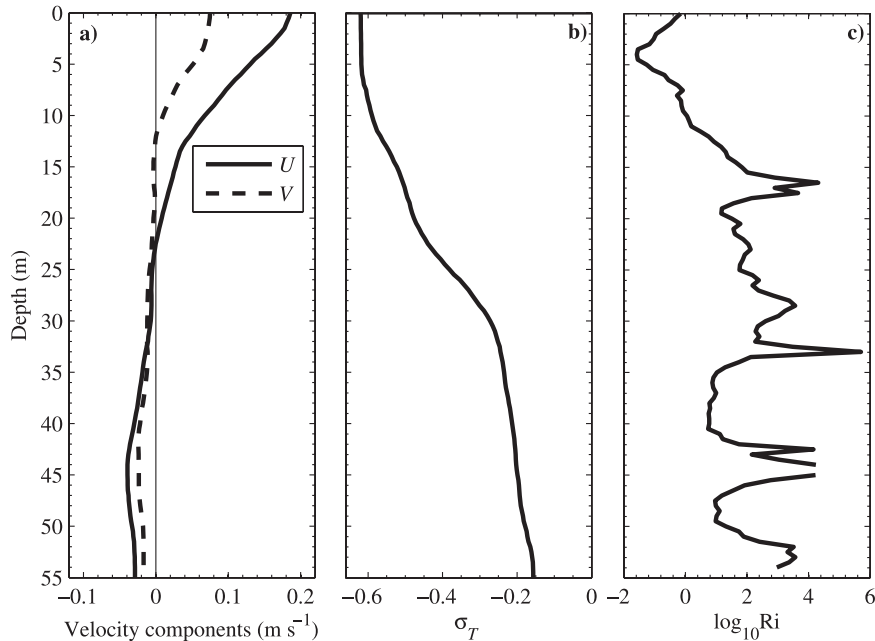


FIG. 1. Profiles, all vs depth  $z$  of mean (a) downwind velocity  $U(z)$  and across-wind velocity  $V(z)$  (to the right of the wind), (b) density  $\sigma_T(z)$ , and (c) logarithm of  $Ri$  ( $\alpha = 75^\circ$ ).

measurements, is shown in Fig. 1b. Regions of static instability are common in individual density profiles in the upper 20 m, with some 30% of the water column in the upper 8 m being statically unstable (with density increasing upward) throughout the period of observation—evidence of persistent turbulent mixing. The overturning or Thorpe scale  $L_T$  decreases monotonically from about 1.7 m at a depth of 6 m to about 0.2 m at 27 m.

The T–G equation, (1), is solved using both the shooting and the matrix methods for two-dimensional disturbances with wavenumbers  $k$  in directions  $\alpha$  relative to the direction of the Loch axis using the mean velocity in this direction,  $W(z) = U \cos\alpha + V \sin\alpha$ . The boundary condition adopted at the surface,  $z = 0$  m, is that the vertical velocity is zero. At the lower end of the measured data,  $z = h = 55$  m, the vertical velocity and the pressure fluctuations are matched to those of an assumed potential flow with uniform density below 55 m. The growth rates and phase speeds determined by the two methods of solving (1) are found to agree to within about 3%, but it proved difficult to maintain convergence using the shooting method at nondimensional wavenumbers  $kh$  greater than 4.5, and the matrix method is therefore used to find the results described below.

The Richardson number on which the two-dimensional disturbances depend varies with direction  $\alpha$ . The profile of  $Ri = N^2/(dW/dz)^2$  at  $\alpha = 75^\circ$  is shown in Fig. 1c. The variation of  $Ri_{\min}$  with  $\alpha$  is shown in Fig. 2. The smallest  $Ri$ , 0.012, is found in the direction  $\alpha = 30^\circ$ .

The growth of periodic disturbances depends also on direction  $\alpha$ , the nondimensional wavenumber  $kh$ , and the mode of the disturbance. Growth rates are calculated for  $0 \leq kh \leq 120$  and  $-15^\circ \leq \alpha \leq 165^\circ$ . The fastest growing mode is mode 1. Growth rates  $kc_i$  are shown as a function of  $kh$  in Fig. 3 in  $15^\circ$  increments of the disturbance direction  $\alpha$  from  $\alpha = 0^\circ$  to  $\alpha = 105^\circ$ . There is generally more than one maximum in  $kc_i$ ; a secondary maximum where  $kh$  is about 5–15, corresponding to a wavelength of 23–69 m, and a larger maximum at a

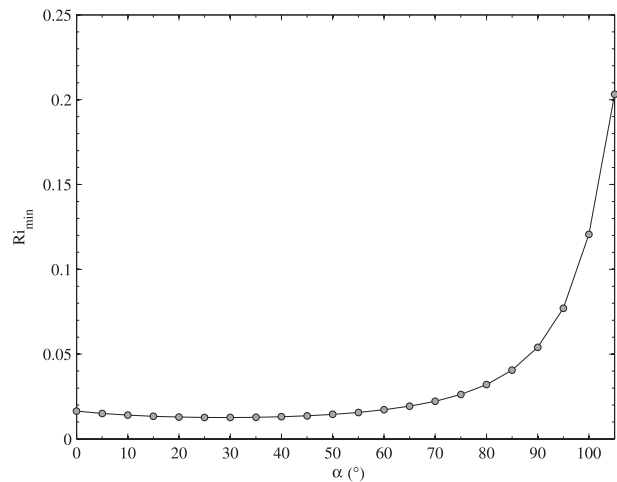


FIG. 2. The minimum values of  $Ri = N^2/(dW/dz)^2$  found in profiles as a function of direction  $\alpha$ .

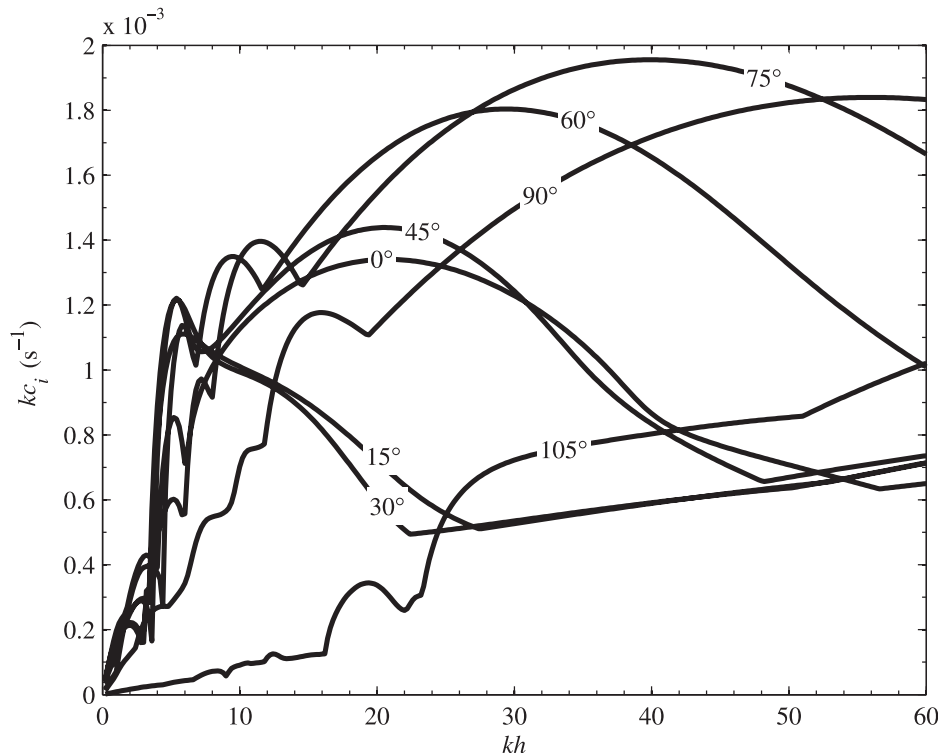


FIG. 3. Growth rates  $kc_i$  of small disturbances as a function of  $kh$  at angles  $\alpha$  from  $0^\circ$  to  $105^\circ$  at  $15^\circ$  intervals.

higher value of  $kh$  corresponding to a smaller wavelength. The fastest growing mode 1 disturbance is found when  $\alpha \approx 75^\circ$  when  $kh = 39.9$  or a wavelength of 8.7 m. The streamfunction  $\phi(z)$  of this disturbance, proportional to the amplitude of the vertical velocity perturbation,  $w = -ik\phi(z) \exp[ik(x - ct)]$ , is shown in Fig. 4 and its maximum at a depth of about 3.5 m. The phase speed of this disturbance is  $0.099 \text{ m s}^{-1}$ , and the “steering” or critical level, where  $c_r = W$ , is approximately at the depth (3.5 m) where the streamfunction is maximum. This is also where  $Ri$  is a minimum and within the region where static instability is frequent.

The maximum growth rate of disturbances is  $1.96 \times 10^{-3} \text{ s}^{-1}$ . The corresponding exponential growth time  $\tau$  is about 8.5 min, giving  $\tau/T_b \approx 0.45$ , where  $T_b = 2\pi N^{-1}$  and  $N \approx 5.5 \times 10^{-3} \text{ s}^{-1}$ , is the mean buoyancy frequency in the upper 10 m of the water column. (This compares with  $\tau/T_{b^*} \approx 1.2$  taking  $T_{b^*} = 2\pi N_{\max}^{-1}$  and using the value,  $N_{\max} \approx 0.015 \text{ s}^{-1}$ , in the thermocline at 25 m; exponential growth occurs within a period  $\tau$ , equal to about 1.2 times the smallest period  $2\pi/N_{\max}$  of internal waves.)

The fastest growing two-dimensional disturbances are not found in the direction for which  $Ri$  is smallest ( $\alpha \approx 30^\circ$ ; Fig. 2) or in the direction ( $\approx 20^\circ$ ) of the near-surface mean flow, but at the greater value of  $\alpha$ , about

$75^\circ$  (Fig. 3). If the across-wind  $V$  component of flow is ignored (as in the earlier calculations described in section 2a) by taking  $\alpha = 0^\circ$ , the largest growth rate is reduced to  $1.34 \times 10^{-3} \text{ s}^{-1}$ , giving  $\tau/T_b \approx 0.65$  or  $\tau/T_{b^*} \approx 1.8$  at  $kh = 20.8$ , a wavelength of 16.6 m.

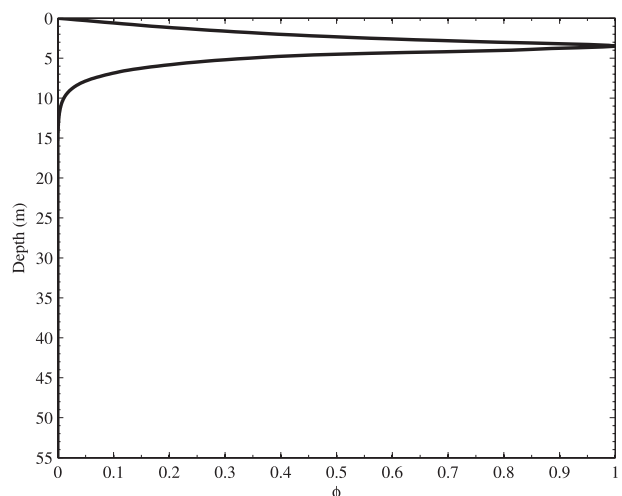


FIG. 4. The streamfunction  $\phi(z)$  proportional to the vertical velocity component, corresponding to the disturbance with maximum growth rate. The function  $\phi(z)$  has been scaled to have a maximum of unity.

The mean velocity of the flow in the direction  $\alpha = 75^\circ$  of the fastest growing disturbances was varied to determine, by extrapolation, the value of  $\Phi$  for which the maximum growth rate is reduced to zero. At this value,  $\Phi$  is about  $-0.78 \pm 0.05$  and using (3),  $Ri_c$  is found by multiplying  $Ri_{\min}$  ( $=0.012$ ) by  $1/(1+\Phi)^2$ , giving  $Ri_c = 0.25 \pm 0.11$  (although the flow must be stable if  $Ri \geq 0.25$  by the Miles–Howard theorem).<sup>6</sup> In this case the value,  $|\Phi|$ , is not much less than unity, implying that the flow is *not* marginal, and  $Ri_c$  is not significantly different from  $1/4$ .

### 3. Conclusions

Several authors (e.g., Thorpe and Hall 1977; Merrill 1977; Sun et al. 1998) have previously used the T–G equation to examine the nature of unstable disturbances and of internal waves in naturally occurring stably stratified shear flows. A novel feature of the present discussion is to address the question, how unstable is an observed flow? and to provide a quantitative answer. The cascading flow (section 1c) is marginal in the sense that  $\Phi = -0.2$  is relatively close to zero, but the analysis of the wind-driven flow in the upper layers of Loch Ness (section 2) finds that  $\Phi = -0.78 \pm 0.05$ ; this refutes the conjecture that turbulent shear flows are generally in a marginal state.

This leaves the further question, why is one flow marginal and another not? There is no very obvious answer. The two boundary layer flows, the marginally unstable cascading flow (section 1c) and the very unstable flow in the mixed layer (section 2; Fig. 1), differ in the way in which they are continuously driven. The former is driven by buoyancy forces and pressure gradients resulting from the downslope component of gravity, and the latter is driven by wind stress transmitted to the water in the presence of surface waves. In both cases the speed of the flow is eventually limited by turbulent Reynolds stresses associated with its instability. The turbulence caused by the instability of flow in the former case may, in the terminology of Turner (1973), be regarded as being driven by an internal process, similar to that of the Mittendorf experiments. The classification of the latter is more ambiguous, since turbulence in the mixed layer may be driven by that caused in breaking surface waves or perhaps by Langmuir cir-

ulation, both “external processes” arising from the waves at the free surface and wind-driven shear. The instability of the mixed layer is, however, best described as an internal mixing process driven by shear, and one that plausibly is a cause of the large-scale intermittent coherent structures found in the mixed layer, the “temperature ramps.” The density and velocity profiles (Fig. 1) and the structure of the fastest growing disturbance (Fig. 4) suggest that, rather than being described as KHI, the instability may best be regarded as a form of asymmetric Holmboe (AH) instability with the greatest shear concentrated in the region above the maximum density gradient (Carpenter et al. 2007). Simple classification is, however, hindered because of the presence of the water surface. [The AH instability accomplishes mixing mainly through entrainment from the upper thermocline, with water being mixed into the upper shear layer and resulting in deepening of the upper mixed layer. This process of entrainment into the mixed layer of Lake Geneva is recorded by Ozen et al. (2006).] The two flows also differ in that the cascading flow evolves spatially, with distance downslope, while the flow in the upper layer of Loch Ness, being at a moderately large fetch (about 20 km), appears to be mainly temporal, the structure of the boundary layer being maintained by a slow upwelling of isopycnals.

The main difference between the flows is in their density, and particularly velocity, profiles. This being so, it appears that no general rule can be drawn to determine how close a given flow is to being marginal within the limits we have chosen to define the term in section 1b; each case may be different and should be judged without the guidance of some general rule. Table 1 summarizes the examples described above, and includes two others. Liu (2009) describes and analyzes the stratified shear flow near the sill at the mouth of the Clyde Sea. One hour, hour 15, of Liu’s analysis when the flow is turbulent, but not in a marginal state, is included in the table. Sun et al. (1998) examine the stability of the flow in the equatorial Pacific where shear results from the presence of the Equatorial Undercurrent. While the zonal component of shear is dominant in the period of observations, there is a substantial meridional shear and energetic oscillations. In a period of 1 h, designated hour 6, the growth rate of the fastest growing disturbance is  $1.1 \times 10^{-3} \text{ s}^{-1}$  for a mode that is maximum at a depth of about 47 m where  $Ri_{\min} = 0.13$  and  $N^2 \approx 0.55 \times 10^{-4} \text{ s}^{-2}$ , giving  $\tau/T_b \approx 1.1$ , close to unity. Since  $0.25 \geq Ri_c \geq Ri_{\min}$ , (3) gives  $-0.28 \leq \Phi \leq 0$ , the value entered in Table 1.

Although the more unstable flows, those with the largest  $|\Phi|$ , have smaller values of  $\tau/T_b$ , the ratio of disturbance growth time to buoyancy period, it is remarkable that in all the examples  $\tau/T_b$  is of order unity. It

<sup>6</sup> As  $\Phi$  decreases from 1.0 to  $-0.2$ , the secondary maximum in  $kc_i$  near  $kh = 10$  diminishes. Maximum growth rate continues to be at  $kh = 39.9$  with a smooth trend of  $\max(kc_i)$  vs  $\Phi$  to  $\Phi = -0.6$ , beyond which extrapolation leads to the stated uncertainty in the value of  $\Phi$  at  $kc_i = 0$ .

appears possible that continuously forced, turbulent flows may not adjust toward a state in which  $Ri_{\min}$  is just less than  $Ri_c$  so that  $\Phi < 0$  and  $|\Phi| \ll 1$ , but to one in which the minimum growth time of disturbances is of the same order as the smallest period of internal waves, the buoyancy period. Sutherland and Linden (1998; see also Sutherland 2001) find that waves near the buoyancy period are generated by, radiate, and drain energy from turbulence in a stratified shear flow. Such waves may be instrumental in transporting energy from the turbulent region, perhaps leading to a physical control, but it is not obvious how this may be quantitatively related to the growth rate of unstable disturbances. It would be of value to examine data from other continuously forced shear flows to see whether  $\tau/T_b \approx 1$ , and to investigate the relation between

the unstable disturbances in a turbulent region and the internal waves radiating from it.

*Acknowledgments.* ZL was in receipt of a scholarship from the China Scholarship Council and partly supported by the Major State Program of China for Basic Research (Grant 2006CB400602).

## APPENDIX

### An Integral Equation for $c$

Moum et al. (2003, their appendix) use the kinetic energy equation to derive an expression for the growth rate of small disturbances as

$$\left\langle \int [U' \partial \psi / \partial x \partial \psi / \partial z - B \partial \psi / \partial x] dz \right\rangle \left/ \left\langle \int [(\partial \psi / \partial x)^2 + (\partial \psi / \partial z)^2] dz \right\rangle \right.,$$

where  $U' = dU/dz$ ,  $B = -g\rho/\rho_0$  is the buoyancy associated with density fluctuations  $\rho$  and the streamfunction is  $\psi(x, z, t)$ , with velocity components  $u = \partial \psi / \partial z$  and  $w = -\partial \psi / \partial x$ . (Moum et al. adopt a convention for  $\psi$  with the negative of the sign used here.) The angle brackets  $\langle \rangle$  denote averaging over one wavelength in  $x$ , averaging accidentally omitted by Moum et al. (Dr. W. D. Smyth 2008, personal communication). The expression is useful in testing the results of the matrix method of solving the T–G equation. We have derived a similar formulation, but one that can be used to check  $c$  when the T–G equation is solved by the matrix method with boundary condition  $\phi(z) = 0$  at rigid boundaries  $z = 0$  and  $h$ , where the vertical velocity,  $w = -\partial \psi / \partial x$ , is zero.

The Taylor–Goldstein equation is given by (1), where  $\phi$  and  $c$  are complex. From the equation of density

conservation, we find an expression for the buoyancy fluctuation

$$b(z) = \frac{\phi N^2}{(U - c)}, \quad (\text{A1})$$

related to the density fluctuation by  $\rho = -(b(z)\rho_0/g) \exp[ik(x - ct)]$ , where  $\rho_0$  is the mean density. Eliminating  $N^2$  in (1) using (A1), multiplying the resulting equation by  $\phi(U - c)$ , integrating from  $z = 0$  to  $h$ , and applying integration by parts, we obtain

$$-\int U' \phi \phi' dz - \int U \phi'^2 dz + c \int \phi'^2 dz + \int b \phi dz - k^2 \int U \phi^2 dz + ck^2 \int \phi^2 dz + 2 \int U' \phi \phi' dz = 0, \quad (\text{A2})$$

with  $\phi' = d\phi/dz$ . Rearranging we have

$$c = \left\{ \int [U(\phi'^2 + k^2 \phi^2) - b\phi - U' \phi \phi'] dz \right\} \left/ \left[ \int (\phi'^2 + k^2 \phi^2) dz \right] \right., \quad (\text{A3})$$

an equation for the complex speed,  $c = c_r + ic_i$ , in terms of integrals from  $z = 0$  to  $h$ .

Equation (A3) gives both the real and imaginary parts of  $c$ . It only applies, however, when  $\phi(0) = 0$  and  $\phi(h) = 0$ , and therefore not in the case examined in section 2.

## REFERENCES

- Alford, M. H., and M. C. Gregg, 2001: Near-inertial mixing: Modulation of shear, strain and microstructure at low latitude. *J. Geophys. Res.*, **106**, 16 947–16 968.
- Carpenter, J. R., G. A. Lawrence, and W. D. Smyth, 2007: Evolution and mixing of asymmetric Holmboe instabilities. *J. Fluid Mech.*, **582**, 103–132.
- Davis, P. A., and W. R. Peltier, 1976: Resonant parallel shear instability in the stably stratified planetary boundary layer. *J. Atmos. Sci.*, **33**, 1287–1300.
- Davis, R. E., R. de Szoeke, D. Halpern, and P. Niiler, 1981: Variability in the upper ocean during MILE. Part 1: The heat and momentum budgets. *Deep-Sea Res.*, **28**, 1427–1451.
- Ellison, T. H., and J. S. Turner, 1959: Turbulent entrainment in stratified flows. *J. Fluid Mech.*, **6**, 423–448.



- Eriksen, C. C., 1978: Measurements and models of finestructure, internal gravity waves, and wave breaking in the deep ocean. *J. Geophys. Res.*, **83**, 2989–3009.
- Fringer, O. B., and R. L. Street, 2003: The dynamics of breaking progressive interfacial waves. *J. Fluid Mech.*, **494**, 319–353.
- Gregg, M. C., 1976: Temperature and salinity microstructure in the Pacific Equatorial Undercurrent. *J. Geophys. Res.*, **81**, 1180–1196.
- Hazel, P., 1972: Numerical studies of the stability of inviscid stratified shear flows. *J. Fluid Mech.*, **51**, 39–61.
- Howard, L. N., 1961: Note on a paper by John W. Miles. *J. Fluid Mech.*, **10**, 509–512.
- Liu, Z., 2009: Instability of baroclinic tidal flow in a stratified fjord. *J. Phys. Oceanogr.*, in press.
- Merrill, J. T., 1977: Observation and theoretical study of shear instability in the airflow near the ground. *J. Atmos. Sci.*, **34**, 911–921.
- Miles, J., 1961: On the stability of heterogeneous shear flows. *J. Fluid Mech.*, **10**, 496–508.
- Mittendorf, G. H., 1961: The instability of stratified flow. M.S. thesis, State University of Iowa, 29 pp.
- Monserrat, S., and A. J. Thorpe, 1996: Use of ducting theory in an observed case of gravity waves. *J. Atmos. Sci.*, **53**, 1724–1735.
- Moum, J. N., D. M. Farmer, W. D. Smyth, L. Armi, and S. Vagle, 2003: Structure and generation of turbulence at interfaces strained by internal solitary waves propagating shoreward over the continental shelf. *J. Phys. Oceanogr.*, **33**, 2093–2112.
- Ozen, B., S. A. Thorpe, U. Lemmin, and T. R. Osborn, 2006: Cold-water events and dissipation in the mixed layer of a lake. *J. Phys. Oceanogr.*, **36**, 1928–1939.
- Sun, C., W. D. Smyth, and J. N. Moum, 1998: Dynamic instability of stratified shear flow in the upper equatorial ocean. *J. Geophys. Res.*, **103** (C3), 10 323–10 337.
- Sutherland, B. R., 2001: Finite amplitude internal wave packet dispersion and breaking. *J. Fluid Mech.*, **429**, 343–380.
- , and P. F. Linden, 1998: Internal wave excitation from a stratified flow over a thin barrier. *J. Fluid Mech.*, **377**, 223–252.
- Thorpe, S. A., 1977: Turbulence and mixing in a Scottish loch. *Philos. Trans. Roy. Soc. London*, **A286**, 125–181.
- , and A. J. Hall, 1977: Mixing in upper layer of a lake during heating cycle. *Nature*, **265**, 719–722.
- , and B. Ozen, 2007: Are cascading flows stable? *J. Fluid Mech.*, **589**, 411–432.
- Troy, C. D., and J. R. Koseff, 2005: The instability and breaking of long internal waves. *J. Fluid Mech.*, **543**, 107–136.
- Turner, J. S., 1973: *Buoyancy Effects in Fluids*. Cambridge University Press, 367 pp.
- Zika, J., 2008: The stability of boundary layer flow. 2007 program of study: Boundary layers, WHOI GFD Summer School 2007 Tech. Rep. WHOI-2008-05, 143–170.